

FXYD6 promotes thermal nociception by regulating TRPV1

Hao Luo¹ , Bing Cai^{1,2}, Jing Pan², Hai-Xiang Shi^{3,4}, Kai-Kai Wang^{1,3}, Yan-Qing Zhong¹, Ying-Jin Lu², Lan Bao^{3,4}, Xu Zhang^{1,2,3,5} and Kai-Cheng Li^{2,5} 

Molecular Pain
Volume 17: 1–15
© The Author(s) 2021
Article reuse guidelines:
sagepub.com/journals-permissions
DOI: 10.1177/1744806921992249
journals.sagepub.com/home/mpx



Abstract

FXYD6, an unnecessary auxiliary subunit of Na⁺,K⁺-ATPase, is expressed in the nervous system. However, its functions remain largely unclear. In the present study, we find that FXYD6 is involved in the thermal nociception. FXYD6 was mainly expressed in small-diameter DRG neurons expressing transient receptor potential channel VI (TRPV1). In the *SNS-Cre/Fxyd6^{Fl/Fl}* mice, loss of FXYD6 in these sensory neurons impaired the behavioral responses to noxious heat stimulus and intraplantar injection of capsaicin. The capsaicin-induced and TRPV1-mediated currents were decreased in the FXYD6-deficient DRG neurons. Heterologous expression of FXYD6 could increase the TRPV1 capsaicin-sensitive currents in HEK293 cells. Furthermore, we found that the negatively charged PGDEE motif in C-terminal of FXYD6 is required for the FXYD6/TRPV1 interaction and FXYD6-mediated enhancement of TRPV1. Disrupting the FXYD6/TRPV1 interaction with the TAT-PGDEE peptide could elevate the threshold of thermal nociception. Therefore, FXYD6 maintains the thermal nociception via interacting with TRPV1 channel in nociceptors.

Keywords

FXYD6, TRPV1, DRG, thermal nociception

Date Received: 11 October 2020; Revised 11 January 2021; accepted: 11 January 2021

Introduction

FXYD6 (Phosphohippolin), was firstly found in the hippocampus and cerebellum.^{1,2} FXYD6 belongs to the single-span membrane protein FXYD family.³ FXYD family members are tissue-specific and subunit isoform-specific regulators of Na⁺,K⁺-ATPase (NKA).^{4,5} As an unnecessary auxiliary subunit of NKA, FXYD6 is found to decrease the NKA activity.⁶ According to previous studies, FXYD6 is related to diseases such as pancreatic cancer, cholangiocarcinoma and hepatocellular carcinoma.^{7–10} It is thought to be a candidate gene of schizophrenia, since the human FXYD6 gene is located in Chr11 q23.3 and contains six SNPs related to the schizophrenia.^{11–13} Furthermore, FXYD6 is expressed in type II spiral ganglion neurons, type II taste bud cells and cochlear stria vascularis of inner ear, and maybe involved in gustation, alcohol addiction, hearing and endolymph homeostasis.^{14–17} In addition, one study shows that *Fxyd6* is widely distributed in almost all subnuclei of parabrachial nucleus, a

¹Institute of Neuroscience and State Key Laboratory of Neuroscience, CAS Center for Excellence in Brain Science and Intelligence Technology, University of Chinese Academy of Sciences, Chinese Academy of Sciences, Shanghai, China

²Institute of Brain-Intelligence Science and Technology, Zhangjiang Laboratory, Shanghai, China

³School of Life Science and Technology, ShanghaiTech University, Shanghai, China

⁴State Key Laboratory of Cell Biology, CAS Center for Excellence in Molecular Cell Biology, Institute of Biochemistry and Cell Biology, University of Chinese Academy of Sciences, Chinese Academy of Sciences, Shanghai, China

⁵Shanghai Clinical Research Center, Chinese Academy of Sciences/XuHui Central Hospital, Shanghai, China

Corresponding Authors:

Xu Zhang, Institute of Neuroscience and State Key Laboratory of Neuroscience, Chinese Academy of Sciences, Shanghai 200031, China. Email: xu.zhang@ion.ac.cn

Kai-Cheng Li, Institute of Brain-Intelligence Science and Technology, Zhangjiang Laboratory, 100 Hai Ke Road, Shanghai 201210, China. Email: kcli@scrc.ac.cn



relay center for sensory information.¹⁸ Therefore, FXYD6 is a widely distributed molecule with varied physiological activities.

Nociception is the protective response of bodies to harmful stimuli.¹⁹ The DRG neurons are pseudo-unipolar neurons, and detect the noxious, thermal, mechanical, and chemical stimuli.²⁰ FXYD6 is expressed in certain subpopulations of primary sensory neurons in the dorsal root ganglion (DRG). The present study is to explore the function of FXYD6 in the nociceptive sensation, because it expressed in one type of mechanoheat nociceptors marked by neuropeptide galanin (Gal).²¹ This type of DRG neurons also express the transient receptor potential channel V1 (TRPV1), which can be activated by noxious heat and its agonist capsaicin.^{22–25} TRPV1 functions can be regulated by Pirt, FGF13, SHANK3, calmodulin and β -Arrestin-2.^{26–30} The function of FXYD6 in somatosensory system remains unknown. It would be interesting to investigate whether FXYD6 could regulate TRPV1 in the DRG neurons.

In the present study, *Fxyd6* was conditionally knock-out (cKO) in the DRG neurons of mice. The mutant mice showed impaired behavioral response to the noxious heat and capsaicin. FXYD6 co-expressed and interacted with TRPV1 in the DRG neurons. The C-terminal PGDEE motif of FXYD6 was required for the FXYD6/TRPV1 interaction and FXYD6-mediated enhancement of TRPV1. FXYD6 could increase the capsaicin-sensitive currents via TRPV1 in the DRG neurons. Furthermore, blocking the FXYD6-TRPV1 interaction elevated the threshold of thermal nociception. Therefore, our study revealed that FXYD6 played an important role in thermal nociception by interacting with TRPV1 channel.

Materials and methods

Animals

Experiments were performed according to the guidelines of the Committee for Research and Ethical Issues of the International Association for the Study of Pain and were approved by the Committee of Use of Laboratory Animals and Common facility, Institute of Neuroscience, Chinese Academy of Sciences. C57BL/6J mice purchased from Shanghai Laboratory Animal Center, Chinese Academy of Sciences (Shanghai, China). *Fxyd6* floxed mice (*Fxyd6^{F/F}*) were generated by adding two loxP sites between upstream of the *Fxyd6* exon 3 and downstream of exon 5. The *Fxyd6* gene was deleted selectively in DRG neurons by crossing *Fxyd6^{F/F}* mice with BAC transgenic mice expressing Cre recombinase controlled by promoter elements of the *Nav1.8* gene, which is mainly expressed in small DRG neurons (*SNS-Cre*). *Fxyd6* cKO mice were viable and

fertile. Mice were raised together with littermates in pathogen-free environment and their health status was routinely checked. No more than 6 mice were housed in one cage. All animals were housed under a 12-h light/dark cycle at 22–26°C, with *ad libitum* access to water and chow. Experiments were conducted during the light phase of the cycle. 2- to 4-month-old male mice were used for all *in vivo* and *in vitro* experiments.

Genotyping

The *Fxyd6* cKO mice were identified by genotyping. A small piece of mouse tail or ear was digested in Proteinase K buffer. The genomic DNA was extracted with phenol/chloroform, precipitated with isopropanol, washed with 75% ethanol and dissolved in water. The mouse genotype was then identified by PCR. The primers for the identification of *Fxyd6* loxP were 5'-ATTCTGGCCATTTCAGACATTAGG-3' and 5'-CAAAGGGGAAACTGAGACCAA-3'. The primers for the identification of *SNS-Cre* were 5'-ATTTGCCTGCATTACCGGTC-3' and 5'-GCATCAACGTTTCTTTTCGG-3'. *Fxyd6* cKO male mice carrying *Fxyd6* loxP and *SNS-Cre* (*SNS-Cre⁺/Fxyd6^{F/F}*, *Fxyd6^{SNS}*) were used as the experimental group, while the male mice carrying *Fxyd6* loxP without *SNS-Cre* (*SNS-Cre⁻/Fxyd6^{F/F}*) were used as the control group.

Plasmid construction

Mouse *Fxyd6* and *Fxyd6* mutants were subcloned into pcDNA3.1myc-His(+)A vector for Co-IP. Mouse *Fxyd6* was subcloned into pIRES2-EGFP vector for electrophysiological recording. Mouse *Trpv1* and mCherry sequences were subcloned and fused into pcDNA3.1-His(+)A vector (Myc-tag deleted) for Co-IP and electrophysiological recording. FXYD6-myc was constructed by PCR amplified the full length cDNAs of mouse FXYD6 with the following 5' and 3' primers: 5'-CCCAAGCTTGGGCCACCATGGAGACGGTGC TGGTC-3' and 5'-CCGGAATTCGTTCTCTGCCT TCTGGGGCTCCG-3' and cloned into pcDNA3.1myc-His(+)A plasmid. The FXYD6 mutants were constructed with KOD and DPNI enzyme. KOD enzyme as a high fidelity enzyme amplified the whole plasmid. DPNI enzyme was used to cleave the methylated plasmid from the E.coli and the mutant plasmid were left. FXYD6 mutant-Myc plasmids were constructed by PCR mutated the different regions of FXYD6-myc with the following 5' and 3' primers: FXYD6 PGDEEmut-Myc: 5'-GCGGCTGCCAGGTGGAGA ACCTCATCACT-3' and 5'-AGCTGCGGCAGCCC TGGGCTTCTGATTGAAACT-3'; FXYD6 PFXYD Ymut-Myc: 5'-GCGGCAGCTCAGACCCTG AGGATTGGGGGGT-3' and 5'-GGCAGCTGCAT

CCTTTTCTTTCTCCTTCTCAGCTGC-3'; FXYD6 (PFXYDY+PGDEE)mut-Myc plasmid was constructed by PCR mutated the PGDEE region of FXYD6 PFXYDYmut-Myc with the following 5' and 3' primers: 5'-GCGGCTGCCAGGTGGAGAACCTCATCACT-3' and 5'-AGCTGCGGCAGCCCTGGGCTTCTGATTGAAACT-3', and cloned into pcDNA3.1-His(+) A vector. TRPV1-Flag-p2A-mCherry was constructed as following. Firstly, TRPV1-Flag and mCherry sequences were amplified by PCR with the primers for TRPV1-Flag: 5'-ATGGAGAAATGGGCTAGCTTAGACT-3' and 5'-AGTTAGTAGCTCCGCTTCCCTTGTCGTCGTCATCCTTGTAGTC-3', and the primers for mCherry: 5'-GGAGGAGAACCCTGGACCTATGGTGAGCAAGGGCGAGGA-3' and 5'-AGCTAGCCCATTCTCCATGGTGGCGGTACCAAGCTTAC-3'. p2A sequence was obtained from the denatured and annealed primers: 5'-GGAAGCGGAGCTACTAAGCTTCCAGCCTGCTGAAGCAGGCTGGAGACGTGGAGGAGAACCCTGGACCT-3' and 5'-AGGTCAGGGTTCTCCTCCACGTCTCCAGCCTGCTTCCAGCAGGCTGAAGTTAGTAGCTCCGCTTCC-3'. Next, pcDNA3.1-His(+)A vector was linearized by PCR amplified. Then TRPV1-Flag, mCherry and p2A sequences were fused into pcDNA3.1-His(+)A myc deletion vector by Hieff Clone Enzyme (Hieff Clone™ Plus One Step Cloning Kit).

Cell culture and transfection

HEK293T cells and HEK293 cells were cultured in MEM with 10% fetal bovine serum. The cells were transiently transfected with plasmids using Lipofectamine 2000 reagent (Invitrogen) and were used for the following various experiments 24–48 hr after transfection. For co-immunoprecipitation, FXYD6-Myc, as well as FXYD6 mutants PGDEEmut-Myc, PFXYDYmut-Myc and (PFXYDY+PGDEE)mut-Myc were co-transfected with TRPV1-Flag-p2A-mCherry into HEK293T cells. For electrophysiological recording, FXYD6-EGFP was co-transfected with TRPV1-Flag-p2A-mCherry into HEK293 cells.

Preparation of FXYD6 antibodies

A peptide (CCSFNQKPRAPGDEEAQVENLITNAAEPQKAEN) mapping at the C terminus of mouse FXYD6 was prepared and mixed with Freund's complete adjuvant, and then used to immunize New Zealand rabbits. The immunizations were repeated 3 weeks and 5 weeks later. The sera were taken and stored at -70°C . The antibody specificity was verified by a pre-absorption assay with peptide at 10^{-5} or 10^{-6} M, and the DRG tissue samples of *Fxyd6* cKO mice.

The antibody efficiency was validated in HEK293T cells transfected with FXYD6 plasmids.

In situ hybridization

Lumbar DRGs were dissected from adult male mice and processed for ISH. The primers for the probes for *Fxyd6* mRNA were 5'-CACTTCCCTTTGCGAAGAGC-3' and 5'-GGAGATGGAGGTCACAGGAG-3'; the primers for *Ii31ra* mRNA were 5'-AGGAAGGTGCGATTGTTGTGG-3' and 5'-GCAGGGTTGGGAACATCAGG-3'; the primers for *Mrgprd* mRNA were 5'-CAAGACAATCCCTCATAGACACG-3' and 5'-GAAGGAGGGTGGTAAGGGTTAG-3'; the primers for *Th* mRNA were 5'-AAATTGCTACCTGGAAGGAGGT-3' and 5'-GGGTGGTACCCTATGCATTAG-3'.

For ISH, cRNA riboprobes were labeled with DIG. Fresh sections of DRG were fixed with 4% paraformaldehyde in DEPC-PBS for 20 min, then acetylated and prehybridized in hybridization buffer for 3 h at 67°C . The sections were then incubated with the hybridization buffer containing 1 $\mu\text{g}/\text{ml}$ of the antisense probe for 16 h at 67°C . After hybridization, the sections were incubated in alkaline phosphatase-conjugated sheep anti-DIG antibodies (1:2000; Roche Molecular Biochemicals). The slides were developed in a solution of 1 $\mu\text{l}/\text{ml}$ NBT and 3.5 $\mu\text{l}/\text{ml}$ BCIP in alkaline phosphatase buffer.

For ISH combined with immunostaining, the hybridized sections were incubated with anti-digoxigenin-AP (1:1000) overnight at 4°C . After being washed in TNT (TS7.5, 0.05% Tween 20) and TS8.0 (0.1 M Tris-HCl, pH 8.0, 0.1 M NaCl, and 10 mM MgCl_2), the sections were incubated with HNPP/FR (1:100) in TS8.0. Once the signals were generated, the sections were washed and then processed for immunostaining.

For double fluorescent ISH, one probe was labeled with fluorescein (FITC), whereas the other was labeled with DIG. Both probes were added to the hybridization buffer. After washing and blocking, the sections were incubated with anti-FITC-HRP (1:4000) overnight at 4°C . After washing with TNT buffer, the sections were incubated with TSA-Plus (DNP, 1:100) for 10 min. Then, the sections were washed with TNT and incubated with anti-DIG-AP (1:1000) and anti-DNP Alexa488 (1:500) in 1% blocking reagent overnight at 4°C . The sections were washed with TNT and TS8.0, and then were developed with HNPP/FR (1:1:100) in TS8.0.

Immunostaining

Adult male mice were fixed with 4% paraformaldehyde and 1% picric acid. L4 and L5 DRGs were dissected and post-fixed for 2 h. Then the tissues were dehydrated and embedded for cryostat sectioning. Cryostat sections of

DRGs were processed for double-immunofluorescent staining or ISH combined with immunostaining. The cryostat sections were incubated in primary antibodies at 4°C overnight, and then incubated in secondary antibodies at 37°C for 45 min.

The primary antibodies against FXYD6 (1:2000, Rb, this paper), TRPV1 (1:500, Go, Santa Cruz, sc-12498), TH (1:1000, Sh, Merk/Millipore, AB1542), NF200 (1:2000, Mo, Sigma, N2912), CGRP (1:500, Go, AbD, 1720–9007), Peripherin (1:500, Rb, Chemicon, AB1530), and Nav1.8 (1:1000, Rb, Alomone Labs, ASC-016). The secondary antibodies were FITC, Cy3 or Cy5-conjugated donkey against goat, rabbit, Mo, or sheep antibodies (1:100; Jackson ImmunoResearch). To label IB4-positive neurons, cryostat sections of DRG were first incubated with 5 µg/ml IB4 (Vector Laboratories), and then were stained with goat antibodies against GSL (1:1000, Go, Vector Lab, AS-2104), followed by FITC-conjugated donkey secondary antibodies against goat (1:100; Jackson ImmunoResearch). The tissues were examined under a confocal microscope.

Co-immunoprecipitation and immunoblotting

The DRGs or transfected HEK293T cells were lysed in ice-cold cell lysis buffer (50 mM Tris, 150 mM NaCl, 0.1% Triton X-100, 10% glycerol, 0.5 mg/ml BSA, 1 mM PMSF, 10 mg/ml aprotinin, 1 mg/ml pepstatin and 1 mg/ml leupeptin) or (10 mM HEPES (pH 7.5), 10 mM NaF, 120 mM NaCl, 5 mM EDTA, 1% Triton X-100, 1 mM PMSF, 10 mg/ml aprotinin, 1 mg/ml pepstatin and 1 mg/ml leupeptin). The suspended lysate was immunoprecipitated with 0.5 µg Rb anti-FXYD6 antibodies or 0.5 µg rabbit antibodies against Flag (Rb, Sigma, F7425) overnight at 4°C and then with protein G-Agarose beads for 1 h at 4°C. Immunoprecipitates in the beads were collected. The sepharose was resuspended in ice-cold cell lysis buffer and incubated in sample buffer (50 mM Tris-HCl, pH 7.4, 2% SDS, 5% β-mercaptoethanol, 10% glycerol, 0.01% bromophenol blue) for 20 min at 60°C. Then the immunoblotting was processed.

The immunoprecipitated samples and 3% of the lysate were loaded for SDS-PAGE, transferred, probed with antibodies and visualized with enhanced chemiluminescence. The antibodies against FXYD6 (1:500, Rb, this paper), TRPV1 (1:500, Go, Santa Cruz, sc-12498), Actin (1:100000, Mo, Chemicon, MAB1501), Flag (1:2000, Rb, Sigma, F3165), Myc (1:2000, Rb, Proteintech, 16286–1-AP), and Myc (1:2000, Rb, Sigma, C3956) were used.

Electrophysiological recording

Whole-cell voltage-clamp recordings were performed to record the capsaicin-induced currents in dissociated small DRG neurons and transfected HEK293 cells. L4 and L5 DRGs of mice were dissected and digested with collagenase (1 mg/ml), trypsin (0.4 mg/ml) and DNase (0.1 mg/ml) in DMEM for 30 min at 37°C. After trituration, freshly dissociated DRG neurons were plated on coverslips and incubated in the ECS (150 mM NaCl, 5 mM KCl, 5 mM CaCl₂, 1 mM MgCl₂, 10 mM HEPES, 10 mM D-glucose, pH 7.34) for at least 1 h. Transfected HEK293 cells were plated on coverslips and could be identified by EGFP and mCherry fluorescence. Only one neuron or one HEK293 cell was tested per coverslip. Capsaicin was used as agonist of TRPV1.

The whole-cell configuration was obtained in voltage-clamp mode. In brief, we filled a glass electrode (resistance of 3–6 MΩ) with intracellular solution and advanced it quickly to the target depth under moderate positive pressure. The pipette solution contained (in mM) 135 K-gluconate, 0.5 CaCl₂, 2 MgCl₂, 5 KCl, 5 EGTA, 5 HEPES and 5 D-glucose. When the tip of the electrode was close to a neuron, the tip resistance was increased. We removed the positive pressure and applied negative pressure to aid in seal formation. We achieved the whole-cell configuration using brief bursts of negative pressure to rupture the cell membrane. For the recording of capsaicin-induced currents, dissociated small DRG neurons and HEK293 cells were held at –60 mV in voltage-clamp mode. The translucent and brilliant small DRG neurons, and transfected HEK293 cells containing EGFP and mCherry fluorescence were patched and recorded. Whole-cell recordings were performed using the Axopatch 200B amplifier, digitized using the Digidata 1440A interface, and controlled using pCLAMP10.1 software. Inward currents induced by capsaicin were recorded and analyzed. Statistical comparisons were made using unpaired Student's t test and differences were considered significant at $p < 0.05$.

Preparation of single DRG neurons and single-cell PCR

After electrophysiological recording, the individual DRG neurons were gently transferred into lysis buffer and processed for single-cell RNA extraction and reverse transcription within 1 h and were subjected to cDNA amplification, according to the manufacturer's protocol (Superscript III, Invitrogen). Subsequently, cDNA was used in separate PCR reactions. The reaction mixture (20 µl) was amplified using ExTaq (Takara) for 45 cycles. Then, we performed PCR to detect the gene expression level of *Fxyd6*, *Trpv1* and *Gapdh*, as well as cell type markers, including *Gal*, *Sst*, *Th*, *Mrgpra3*, and *Mrgprd*. The PCR products were analyzed on

ethidium bromide-stained 1.5% agarose gels. Recorded neurons were sorted into corresponding clusters.

The single-cell PCR primers for *Fxyd6* were 5'-CAGACCCTGAGGATTGGG-3' and 5'-CGCAGCGTTTGTAGTGATG-3'; primers for *Trpv1* were 5'-CCCTATCATCACCGTCAG-3' and 5'-TCCAGGAGCAGAGCAAT-3'; primers for *Gapdh* were 5'-GTTGTCTCCTGCGACTTCA-3' and 5'-GGTCCAGGGTTTCTTACTCC-3'; primers for *Gal* were 5'-CAGTAAGCGACCATCCAG-3' and 5'-ATCCCAAGTCCCAGAGTG-3'; primers for *Sst* were 5'-TGGCTTTGGGCGGTGTCA-3' and 5'-CCATTGCTGGGTTTCGAGTT-3'; primers for *Th* were 5'-TTCTGGAACGGTACTGTGGC-3' and 5'-TCGGGTGAGTGCATAGGTGA-3'; primers for *Mrgpra3* were 5'-ACCATTATTTCAATTACTC-3' and 5'-AGTACAAACACACCAGGTGC-3'; primers for *Mrgprd* were 5'-TGGCATCCCAACAAACAC-3' and 5'-CACATCCACCCAGTAGAGTAAG-3'.

Behavioral tests

All experiments were carried out in accordance with the guidelines of the Committee for Research and Ethical Issues of the International Association for the Study of Pain, and approved by the Committee of Use of Laboratory Animals and Common facility, Institute of Neuroscience, CAS.

Adult male animals were housed under a 12:12 h light/dark cycle at 22–26°C, and tests were performed blind to genotype. In the Hargreaves and hot plate tests, the response latency to nociceptive stimuli was measured. In von Frey test, the threshold of nociceptive responses was measured. The tests above were stopped at a cut-off time or force for animal protection.

To examine heat sensitivity of the hindpaw, the mice were placed and habituated in plastic chambers on the surface of a glass plate. The radiant light was applied to one of their hindpaws using a radiant heat stimulator (Ugo Basile, 37,370 Plantar Test, Hargreaves Apparatus). The radiant light was applied when the mice were resting quietly and was stopped immediately after the movement of the hindpaw. The latency was determined as the duration from the beginning of the heat stimulus to the occurrence of a hindpaw withdrawal reflex. The cut-off time was 20 s.

The hotplate test was performed by using a hotplate (Ugo Basile, 35,100 Hot/Cold plate) maintained at 52°C. The response latency was determined by observing the signs of nociception, such as jumping or licking of a paw. The cut-off times at 52°C was 45 s.

In the von Frey test, the mice were habituated in plastic chambers on a mesh floor. Mechanical stimuli were applied using ascending graded individual monofilaments. A von Frey filament was applied 5 times to

each testing site of the hindpaw. The bending force of the von Frey filament to evoke paw withdrawal with over 50% occurrence frequency was determined as the mechanical threshold.

Capsaicin solution was injected into the left hindpaw of mice. The licking and lifting time of the injected hindpaw during 10 min after injection was recorded and analyzed.

PGDEE Scramble sequence was obtained from the online website <http://www.mimotopes.com/peptideLibraryScreening.asp?id=97>. HIV-1 TAT core sequence (YGRKKRRQRRR) is commonly used to help the target protein to penetrate the membrane. HIV-1 TAT-PGDEE (YGRKKRRQRRRPGDEE) and TAT-Scramble (YGRKKRRQRRRREGDPE) were synthesized in GL Biochem (Shanghai) Ltd and then were dissolved well in double-distilled water as stocks (100 mM). In the hotplate test, the mice were habituated and measured the basal threshold. Then the mice were held and intrathecally injected with 10 µl saline or TAT peptide diluted in saline (containing 3 µg peptide). After recovery, the mice were measured the thermal latency from 1 hr to 8 hrs after intrathecal injection.

Statistical analysis

The data are presented as mean ± SEM. Sample number (n) values are indicated in figures, figure legends or results section. Two groups were compared by a two-tailed, unpaired Student's t test. Comparisons among multiple groups were performed by using two-way ANOVA with Bonferroni's post hoc test. Statistical analysis was performed using PRISM (GraphPad Software). Differences were considered significant at $p < 0.05$ (* $p < 0.05$, ** $p < 0.01$, *** $p < 0.001$ and N.S. not significant).

Results

Fxyd6 is mainly expressed in small-diameter DRG neurons

Analysis on our scRNA-seq data showed that *Fxyd6* was mainly expressed in the C1 type DRG neurons marked by *Gal* and the C3 type neurons marked by *Th* (Figure 1 (a)). *Fxyd6* was present in about 23.5% of DRG neurons, and they were small-diameter DRG neurons (cross-sectional area of neuron profiles < 600 µm²) (Figure 1(b) and (c)). Double *in situ* hybridization (ISH) or ISH combined with immunostaining showed that in the lumbar 4 and 5 DRGs of mice, almost all *Fxyd6* expressed in all *Th*-positive neurons and in peripherin-positive (a classical marker of most small-diameter DRG neurons) neurons, but not co-expressed with marker gene *Il31ra* or *Mrgprd* for C2 or C5 types of

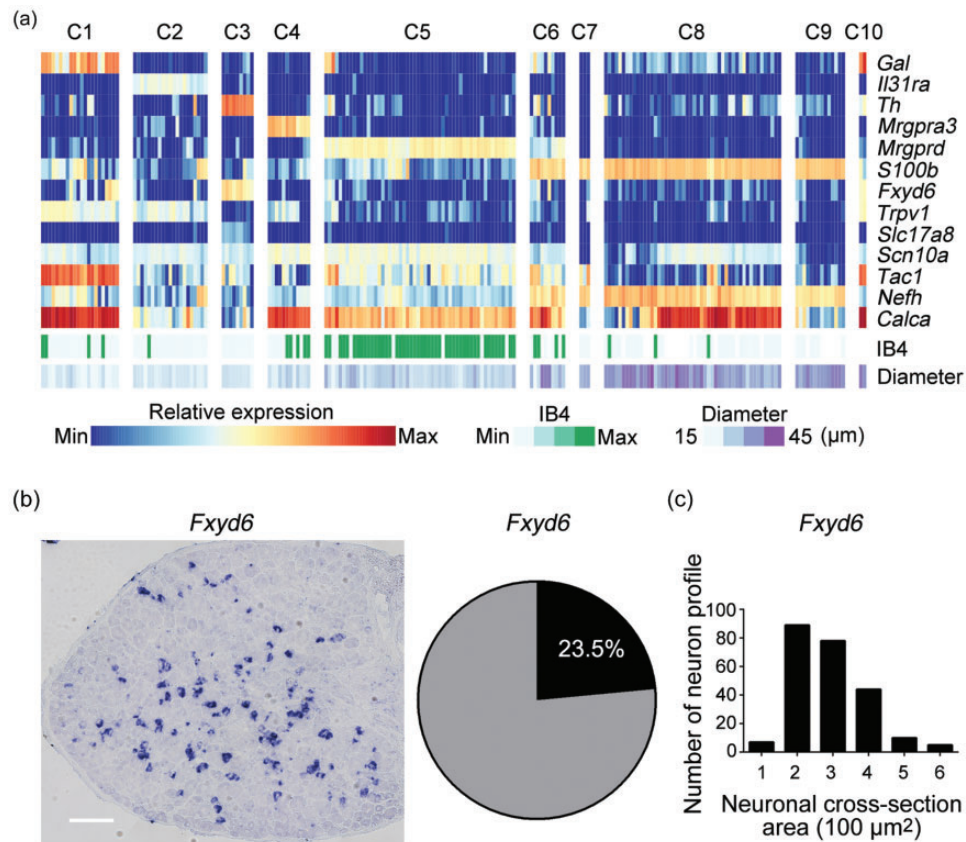


Figure 1. *Fxyd6* is expressed in small DRG neurons. (a) Different genes have distinct expression patterns in the mouse DRG neurons. Based on the single-cell RNA-seq data, DRG neurons could be classified into 10 types, namely C1-C10. A heatmap showed that each type has its own corresponding markers, such as *Gal* for C1, C2 *Il31ra*, C3 *Th*, C4 *Mrgpra3*, and C5 *Mrgprd*. As demonstrated, *Fxyd6* was mainly expressed in small DRG neurons, especially in the C1 *Gal*⁺ and C3 *Th*⁺ type neurons. The ranges of the relative expression levels of different genes, and the range of IB4-labeling and the diameter of each type of neurons are presented with colors indicated in the last panel. (b) ISH result demonstrates that *Fxyd6* is present in about 23.5% of DRG neurons. (c) The statistical results demonstrated that the *Fxyd6* mRNA-containing neurons were small-diameter DRG neurons (cross-sectional area of neuron profiles < 600 μm²).

small DRG neurons, respectively. Double-immunostaining showed that FXYD6 was mainly distributed in the GAL or TH-positive small DRG neurons, and a few IB4-positive small DRG neurons, but not in NF200-positive large DRG neurons (Figure 2).

FXYD6 protein is transported to the afferent fibers in the superficial laminae of the spinal cord

The expression profile of FXYD6 in the nervous systems of adult mice was also examined, and immunoblotting showed that FXYD6 was widely distributed in the hippocampus and cerebellum as reported previously, as well as in the DRG and spinal cord (Figure 3(a)). However, in the lumbar 4 and 5 segments of spinal cord, ISH showed that *Fxyd6* was not detected in the superficial laminae (Figure 3(b)). Double-immunostaining showed that in the lamina I and II of spinal cord, FXYD6 was present in the nerve fibers positive for neuropeptides substance P (SP) and CGRP, two

classical markers of the superficial laminae of the spinal dorsal horn. Moreover, FXYD6 was not found in the PKCγ-containing local neurons of spinal dorsal horn (Figure 3(c)). Thus, FXYD6 is predominantly expressed in the small-diameter DRG neurons, and then could be transported to their afferent fibers in the superficial laminae of the spinal cord.

Fxyd6 cKO mice have impaired behavioral responses to noxious heat

Given that FXYD6 is expressed in C1 type of small DRG neurons and present in their afferent fibers in the superficial layers of spinal cord, FXYD6 might play a potential role in the somatosensory regulation. To examine the FXYD6 function, we generated *Fxyd6* floxed mice (*Fxyd6*^{F/F}), in which two loxP sites were added between upstream of the *Fxyd6* exon 3 and downstream of exon 5. Because Na_v1.8 (SNS, encoded by gene *Scn10a*)-positive neurons could cover the *Fxyd6*-positive neurons, we

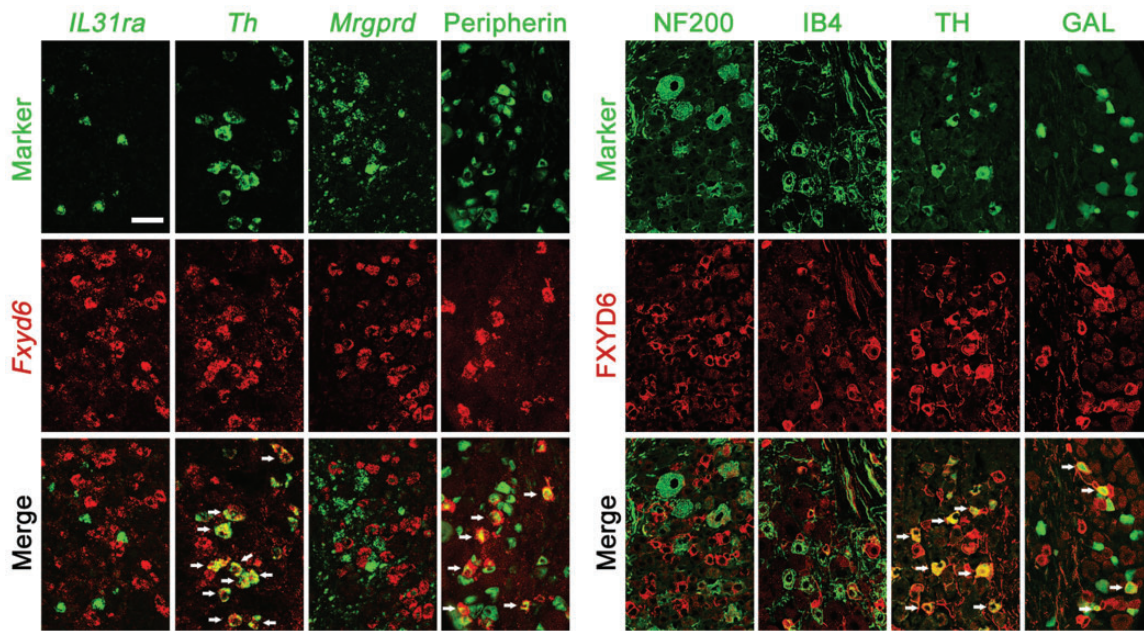


Figure 2. FXYD6 is expressed in two subpopulations of small DRG neurons. Double fluorescent ISH and immunostaining showed the expression of FXYD6/*Fxyd6* and related markers in DRG neurons. *Fxyd6* was mainly co-expressed with peripherin, but not NF200 and IB4 in DRG neurons. FXYD6 was co-expressed with TH and GAL partially. However, *Fxyd6* was not co-expressed with *Il31ra* and *Mrgprd*. Scale bar = 50 μ m.

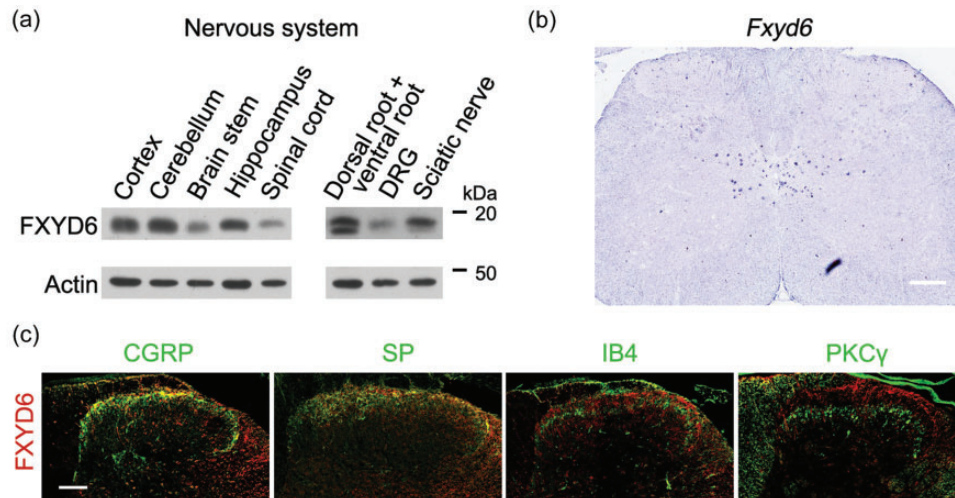


Figure 3. FXYD6 protein is transported to the afferent fibers in the superficial laminae of the spinal cord. (a) Immunoblotting result showed that FXYD6 was widely expressed in nervous system, including cortex, cerebellum, brain stem, hippocampus, spinal cord, dorsal root and ventral root, DRG and sciatic nerve. (b) ISH result demonstrated that *Fxyd6* mRNA was not detected in the superficial laminae of the lumbar 4 and 5 segments of spinal cord. *Fxyd6* mRNA was mainly expressed in the central canal of the spinal cord. Scale bar = 200 μ m. (c) Double fluorescent immunostaining showed that the expression of FXYD6 in spinal cord. FXYD6 was co-localized with CGRP and SP, but not IB4 or PKC γ , in the superficial dorsal horn of lumbar spinal cord. Scale bar = 100 μ m.

crossed the *SNS-Cre* mice with the *Fxyd6*^{F/F} mice to obtain the *Fxyd6* cKO mice, namely *SNS-Cre*/*Fxyd6*^{F/F} (*Fxyd6*^{SNS}) mice (Figures 1(a) and 4(a)). Immunoblotting results showed that FXYD6 level was decreased in *Fxyd6*^{SNS} mice (Figure 4(b)). Then we

carried out a series of behavior tests to study the possible roles of FXYD6 in the somatosensory neurotransmission.

In the Hargreaves test of thermal nociception, *Fxyd6* cKO mice showed elevated paw withdrawal latency,

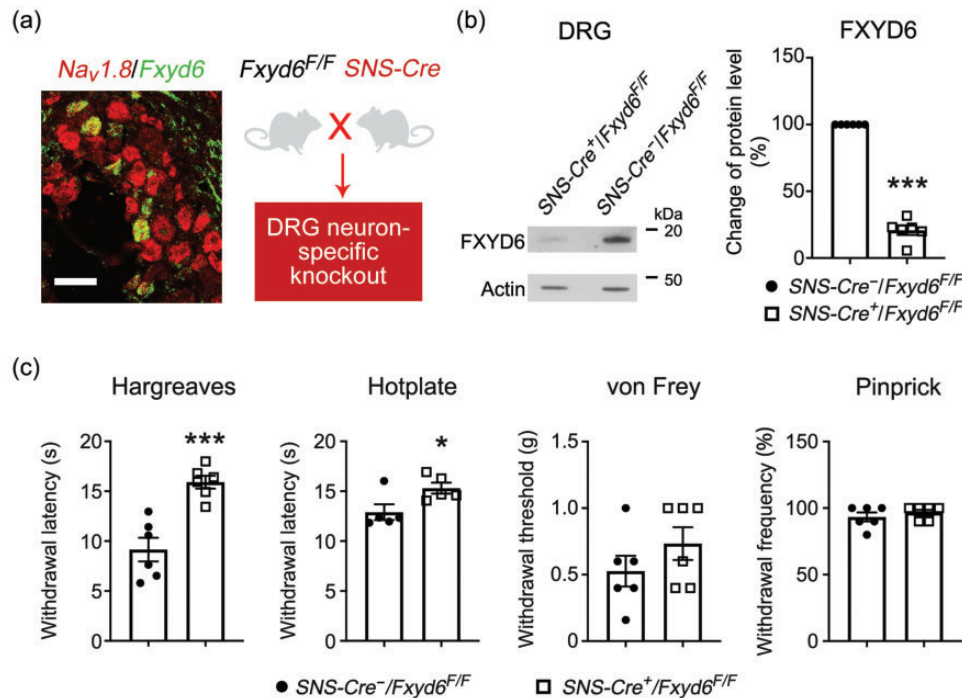


Figure 4. *Fxyd6* cKO mice shows impaired behavioral response to noxious heat. (a) The generation strategy of *Fxyd6* cKO mice. Double fluorescent ISH showed that *Fxyd6* was co-expressed with *Nav1.8* in DRG neurons, so *Fxyd6^{F/F}* mice and *SNS-Cre* mice were crossed to generate *Fxyd6* cKO mice. (b) Immunoblotting showed that the FXD6 level in DRG of *Fxyd6* cKO mice was decreased, compared to that of control mice (** $p < 0.001$, *Fxyd6* cKO mice versus control mice, $n = 6$). Data shown are mean \pm SEM. (c) Hargreaves test showed that the thermal latency of *Fxyd6* cKO mice was increased, compared to that of control mice (** $p < 0.001$, *Fxyd6* cKO mice versus control mice, $n = 6$). Hotplate test showed that the thermal latency of *Fxyd6* cKO mice was increased, compared to that of control mice (* $p < 0.05$, *Fxyd6* cKO mice versus control mice, $n = 5$). Von Frey test showed that the mechanical threshold of *Fxyd6* cKO mice was not significantly altered compared to control mice ($n = 6$ for both *Fxyd6* cKO mice and control mice). Pinprick test showed that the paw withdrawal frequency was unchanged between *Fxyd6* cKO mice and control mice ($n = 6$ for both *Fxyd6* cKO mice and control mice). Data shown are mean \pm SEM.

compared with control mice ($t = 5.006$, $df = 10$, $p = 0.0005$) (Figure 4(c)). In the hotplate test, *Fxyd6* cKO mice also showed elevated paw withdrawal latency at 52°C ($t = 2.503$, $df = 8$, $p = 0.0367$) (Figure 4(c)). However *Fxyd6* cKO mice displayed the comparable mechanical threshold in von Frey test ($t = 1.224$, $df = 10$, $p = 0.2489$) and the normal sensitivity to noxious mechanical stimuli in pinprick test ($t = 0.8452$, $df = 10$, $p = 0.4178$) (Figure 4(c)). Taken together, these results indicated that FXD6 in DRG neurons could regulate the thermal nociception.

FXD6 co-expresses and interacts with TRPV1

We further studied the underlying mechanism for the FXD6-mediated regulation of thermal nociception. We performed intraplantar injection of capsaicin or saline into the hindpaw of *Fxyd6* cKO mice and control mice, and recorded the time spent on licking the hindpaw. Both *Fxyd6* cKO mice and control mice showed little or no responses to the injection of saline ($t = 0.09386$, $df = 8$, $p = 0.9275$) (Figure 5(a)). However, a significant

reduction in the response time was observed in *Fxyd6* cKO mice, compared to control mice ($t = 2.745$, $df = 10$, $p = 0.0207$) (Figure 5(a)). This result largely links TRPV1 channel with the thermal phenotypes found in *Fxyd6* cKO mice. Then, we further studied the relationship between FXD6 and TRPV1, including co-expression and interaction. We found that about 41.9% FXD6-positive neurons expressed TRPV1, while about 19.8% TRPV1-positive neurons expressed FXD6 (Figure 5(b)). Furthermore, Co-immunoprecipitation (Co-IP) results demonstrated that FXD6 could interact with TRPV1 in the DRG (Figure 5(c)). Meanwhile, Co-IP showed in transfected HEK293T cells, FXD6 also interacted with TRPV1 (Figure 5(d)). These data suggest that FXD6 co-expresses and interacts with TRPV1 in C1 type of mechanoheat nociceptors.

TRPV1 function is impaired in FXD6-deficient, Gal⁺ small DRG neurons

The DRG neurons were acutely dissociated and cultured, and small DRG neurons were patch-clamped with

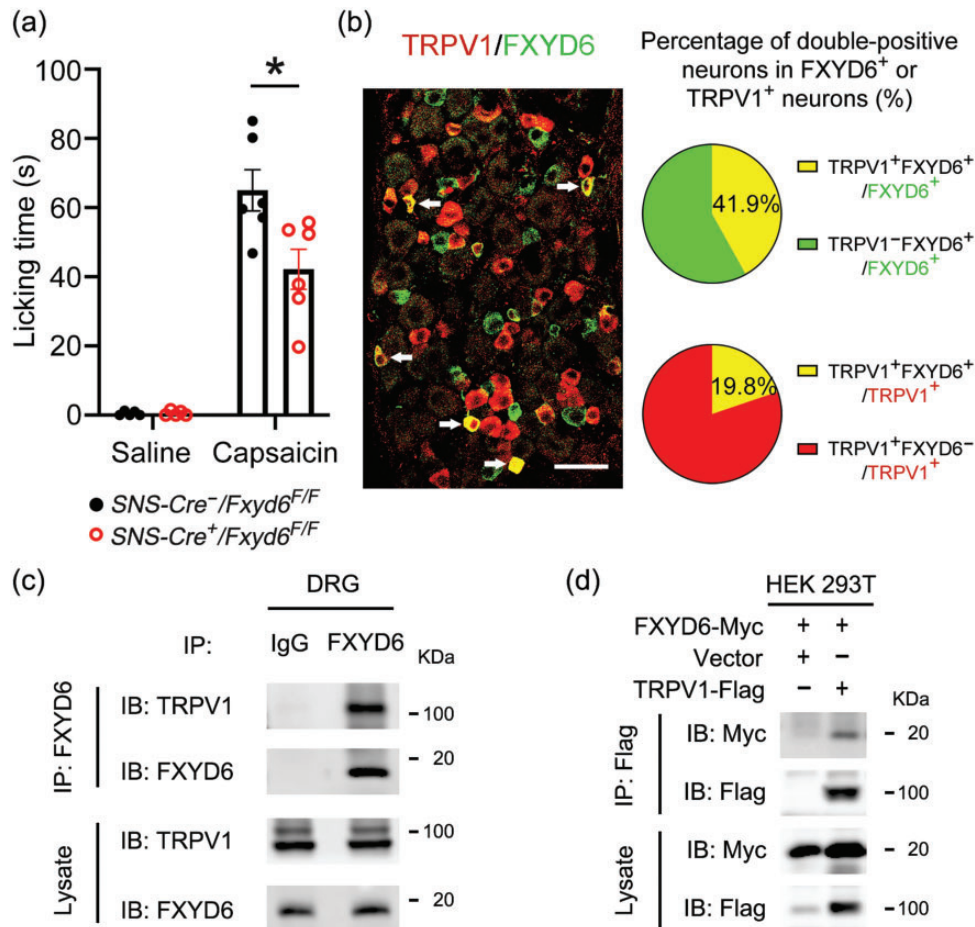


Figure 5. FXYD6 co-expresses and interacts with TRPV1. (a) Intraplantar injection of capsaicin or saline into the hindpaw was performed in *Fxyd6* cKO mice and control mice. Behavioral responses to intraplantar injection of capsaicin or saline were measured for 10 min after injection. Both *Fxyd6* cKO mice and control mice showed little or no responses to the injection of saline ($p = 0.9275$, *Fxyd6* cKO mice versus control mice, $n = 5$). When compared to control mice, the licking time after capsaicin injection was decreased in *Fxyd6* cKO mice ($*p < 0.05$, *Fxyd6* cKO mice versus control mice, $n = 6$). Data shown are mean \pm SEM. (b) Double-fluorescence immunostaining result showed that FXYD6 and TRPV1 co-expressed in small DRG neurons. About 41.9% FXYD6⁺ neurons also expressed TRPV1, while about 19.8% TRPV1⁺ neurons also expressed FXYD6. Scale bar = 50 μ m. (c) Co-IP showed that TRPV1 (~100 kDa) was in the proteins precipitated with the FXYD6 antibody from the mouse DRGs. Three independent experiments were performed with similar results. (d) In the lysate of HEK 293T cells co-transfected with plasmids expressing TRPV1-Flag and FXYD6-Myc, FXYD6-Myc (~20 kDa) was found in proteins precipitated with Flag antibodies. Three independent experiments were performed with similar results.

or without capsaicin treatment. The currents of capsaicin-responsive DRG neurons from *Fxyd6* cKO mice were decreased, compared with control mice ($t = 4.423$, $df = 52$, $p < 0.001$) (Figure 6(a)). After recording, we collected the DRG neurons, extracted total RNA from these neurons and obtained cDNA for single-cell PCR by reverse transcription. Then, we classified these recorded DRG neurons into different types according to the markers of different neuron types detected in these neurons (Figure 6(b)). In the *Gal*⁺ C1 type of DRG neurons, but not *Th*⁺ C3 type of DRG neurons, we found that the capsaicin-induced currents were decreased significantly in the *Trpv1*⁺/*Fxyd6*⁻ neurons, compared to *Trpv1*⁺/*Fxyd6*⁺ neurons ($t = 2.385$, $df = 29$, $p = 0.0238$) (Figure 6(c)). In addition, in

HEK293 cell line, the heterologous expression of FXYD6 could also increase the TRPV1 capsaicin-sensitive currents ($t = 2.030$, $df = 43$, $p = 0.0486$) (Figure 6(d)). These results suggest that FXYD6 could upregulate the TRPV1 activity.

The PGDEE motif of FXYD6 is required for the FXYD6/TRPV1 interaction and FXYD6-mediated enhancement of TRPV1

Taken into the consideration that the mouse FXYD6 protein consisted of 95 amino acids, we tried to screen the key amino acids for the FXYD6/TRPV1 interaction. We aligned the FXYD6 sequences of different species, and focused on the two conserved motifs, namely highly

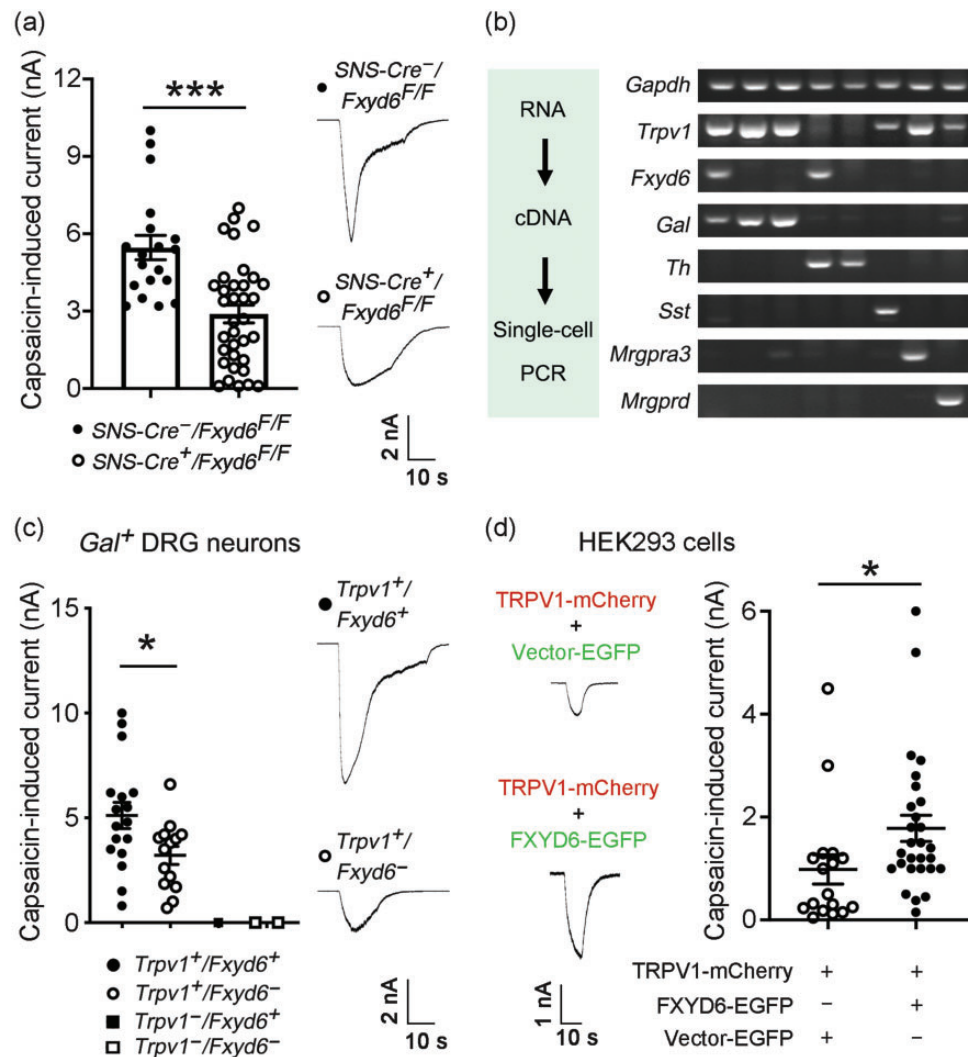


Figure 6. FXYD6 increases the capsaicin-sensitive currents. (a) DRG neurons were dissociated acutely and cultured. The patch-clamp recording of these neurons was performed when capsaicin was applied. The currents of DRG neurons responding to capsaicin (5 μ M) in *Fxyd6* cKO mice were smaller than those in control mice ($n = 19$ for DRG neurons from control mice and $n = 35$ for DRG neurons from *Fxyd6* cKO mice, *** $p < 0.001$ *Fxyd6* cKO mice versus control mice). Data shown are mean \pm SEM. (b) The workflow of electrophysiological studies and single-cell PCR. Small DRG neurons were dissociated acutely, patch-clamped and recorded when capsaicin (5 μ M) was applied for 3 times and 10 seconds per time. Then DRG neurons were collected and total RNA were extracted. The cDNA of neurons were obtained by reverse transcription and processed for the single-cell PCR. Finally, all DRG neurons were classified into different types, according to the neuron type markers detected by single-cell PCR. (c) Single-cell PCR showed that 34 DRG neurons were *Gal⁺* type neurons, in which 3 neurons didn't express *Trpv1* (*Trpv1⁻*) and remaining 31 neurons expressed *Trpv1* (*Trpv1⁺*). Statistical result showed that TRPV1 capsaicin-sensitive currents in the *Trpv1⁺/Fxyd6⁻ Gal⁺* type DRG neurons were smaller, compared to that of *Trpv1⁺/Fxyd6⁺ Gal⁺* type of small DRG neurons ($n = 17$ for *Trpv1⁺* and *Fxyd6⁺* neurons and $n = 14$ for *Trpv1⁺* but *Fxyd6⁻* neurons, * $p < 0.05$, unpaired t test). Data shown are mean \pm SEM. (d) In HEK293 cells, TRPV1-mCherry was co-transfected with FXYD6-EGFP (TRPV1 + FXYD6) or Vector-EGFP (TRPV1 + Vector). FXYD6 could increase the TRPV1 capsaicin-sensitive currents ($n = 26$ for TRPV1 + FXYD6 cells and $n = 17$ for TRPV1 + Vector cells, * $p < 0.05$, unpaired t test). Data shown are mean \pm SEM.

negatively charged PGDEE motif and highly conserved PFXYDY motif (Figure 7(a)). The mouse FXYD6 mutant plasmids were constructed, in which these motifs were replaced with alanine (Ala, A). Co-IP showed that when the PGDEE motif was replaced into neutral amino acid alanine (PGDEEmut), the interaction between the FXYD6 PGDEEmut and TRPV1

were significantly decreased ($t = 7.787$, $df = 8$, $p < 0.0001$ versus the PGDEEmut and FXYD6 CDS, $n = 5$; $t = 1.666$, $df = 10$, $p = 0.1267$ versus the PFXYDYmut and FXYD6 CDS, $n = 6$; $t = 1.745$, $df = 6$, $p = 0.1317$ versus the (PF+PG)mut and FXYD6 CDS, $n = 4$) (Figure 7(b) and (c)). The PGDEE motif, which is completely conserved in all FXYD6 sequences

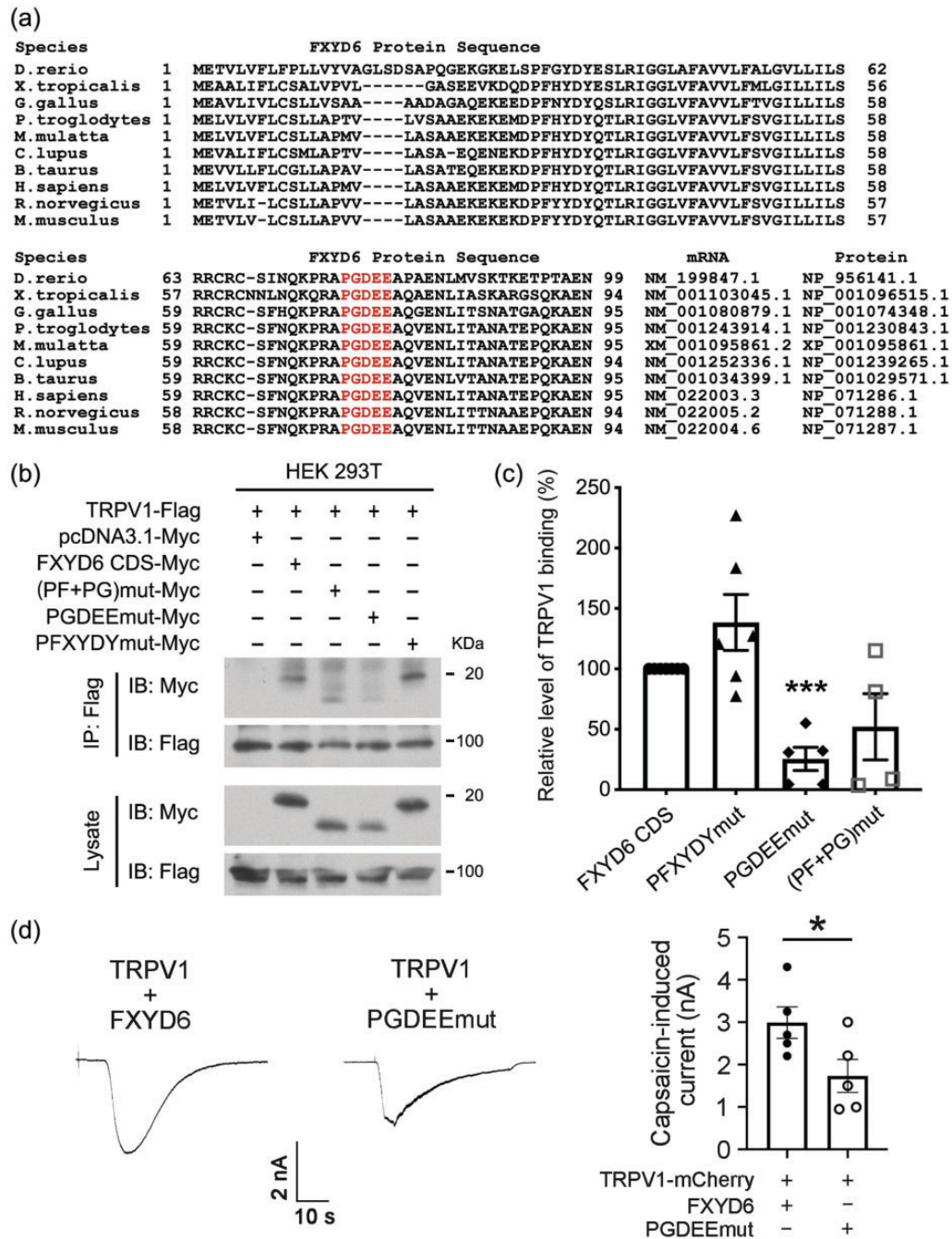


Figure 7. The PGDEE motif of FXYP6 is required for the FXYP6/TRPV1 interaction. (a) Alignment of FXYP6 protein sequences of different species indicated the PGDEE motif was completely conserved. (b) In the lysate of HEK 293T cells co-transfected with the plasmids expressing TRPV1-Flag and FXYP6-Myc or FXYP6mut-Myc, Co-IP showed that FXYP6-Myc or FXYP6mut-Myc is present in the proteins precipitated by Flag antibodies. The immunoblot signal of PGDEEmut-Myc was weaker than that of FXYP6 CDS-Myc in cells co-expressing TRPV1-Flag. The immunoblot shown are representatives of four such experiments. (c) Quantitation showed that the interaction between PGDEEmut-Myc and TRPV1-Flag was weaker than that between FXYP6 CDS-Myc and TRPV1-Flag ($t = 7.787$, $df = 8$, $***p < 0.0001$, PGDEEmut versus FXYP6 CDS, $n = 5$; $t = 1.666$, $df = 10$, $p = 0.1267$, PFXYP6mut versus FXYP6 CDS, $n = 6$; $t = 1.745$, $df = 6$, $p = 0.1317$, (PF+PG)mut versus FXYP6 CDS, $n = 4$). (d) In HEK293 cells, TRPV1-mCherry was co-transfected with FXYP6 (TRPV1 + FXYP6) or PGDEEmut (TRPV1 + PGDEEmut). The TRPV1 capsaicin-sensitive currents in the PGDEEmut group were significantly decreased when compared to those in the FXYP6 group ($n = 5$ for both TRPV1 + FXYP6 cells and TRPV1 + PGDEEmut cells, $*p < 0.05$, unpaired t test). Data shown are mean \pm SEM.

of different species, displays its important role in mediating the FXYD6/TRPV1 interaction.

Next, we further wondered that the PGDEE motif of FXYD6 is indispensable for the FXYD6-mediated enhancement of TRPV1 or not, here we still used the HEK293 cell line, and we co-transfected TRPV1-mCherry with FXYD6 (TRPV1 + FXYD6) or PGDEEmut (TRPV1 + PGDEEmut) in the HEK293 cell line. The TRPV1 capsaicin-sensitive currents in the PGDEEmut group were significantly decreased when compared to those in the FXYD6 group found ($t = 2.342$, $df = 8$, $p = 0.0473$) (Figure 7(d)). These results suggest that PGDEE motif is also required for the FXYD6-mediated enhancement of TRPV1.

TAT-PGDEE elevates the threshold of response to the noxious thermal stimulation

As FXYD6 could interact with TRPV1 channel via its PGDEE motif, we wondered whether the PGDEE motif was also involved in thermal nociception. Taking advantage of cell-penetrating peptide HIV-1 TAT (GRKKRRQRRRPQ), we designed the TAT-PGDEE, and the corresponding TAT-PGDEE scramble peptide (TAT-Scramble). Then the wildtype mice were intrathecally injected with the TAT peptides or saline. Hotplate test showed that TAT-PGDEE could elevate the thermal threshold in C57 mice, but TAT-Scramble or saline could not change the thermal threshold ($F_{(1,128)} = 28.36$, $p < 0.0001$ versus the TAT-PGDEE group and the TAT-Scramble group; $F_{(1,112)} = 20.83$, $p < 0.0001$ versus the TAT-PGDEE group and the Saline group; $n = 11$ for TAT-PGDEE group, $n = 7$ for the TAT-Scramble group and $n = 5$ for the Saline group) (Figure 8). Therefore, the PGDEE motif of FXYD6 is not only required for the FXYD6/TRPV1 interaction, but also plays an important role in thermal nociception.

Discussion

The present study showed that FXYD6 co-expresses with TRPV1 in *Gal*⁺ C1 type of small DRG neurons. FXYD6 could interact with TRPV1 and increase the capsaicin-sensitive currents via TRPV1. In *Fxyd6* cKO mice, TRPV1 capsaicin-sensitive currents were significantly decreased in *Gal*⁺ C1 type of DRG neurons. *Fxyd6* cKO mice showed impaired behavioral response to noxious heat. The highly negatively charged C-terminal PGDEE motif of FXYD6 was required for the FXYD6/TRPV1 interaction and FXYD6-mediated enhancement of TRPV1, and intrathecal TAT-PGDEE could elevate thermal threshold. These findings reveal that FXYD6 could promote the thermal nociception through regulating TRPV1 activity in a specific type of DRG neurons.

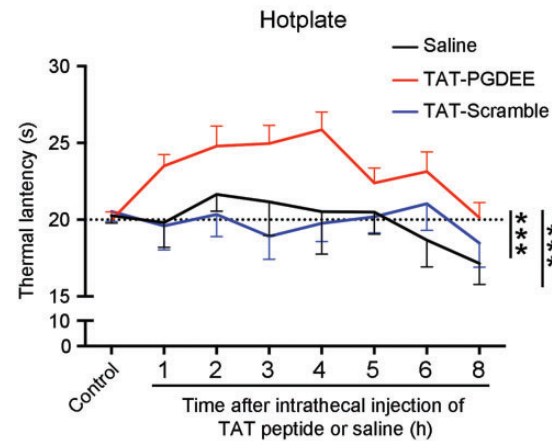


Figure 8. TAT-PGDEE elevates the threshold of response to the noxious thermal stimulation. The mice were intrathecally injected with the TAT-PGDEE, TAT-Scramble or Saline, and then recovered in 30 minutes. TAT-PGDEE could elevate the threshold of response to the noxious thermal stimulation. Hotplate test showed that TAT-PGDEE could elevate the threshold to heat stimulation (52°C), but TAT-Scramble or Saline could not ($n = 11$ for TAT-PGDEE group, $n = 5$ for Saline group, and $n = 7$ for TAT-Scramble group, $***p < 0.001$, versus the indicated group, two-way ANOVA).

FXYD6/TRPV1 interaction involves in thermal nociception

FXYD6 is an unnecessary subunit of Na^+ , K^+ -ATPase, and could decrease the activity of Na^+ , K^+ -ATPase.⁶ Our previous studies demonstrate that secreted protein FSTL1 and membrane protein FXYD2 could regulate Na^+ , K^+ -ATPase activity distinctly, resulting in the alterations of neuronal excitability and threshold of somatosensation.^{31–33} Here, we found that besides the FSTL1/FXYD2/NKA system, the FXYD6/TRPV1 interaction also could play a role in somatosensation. In present study, we found that FXYD6 and TRPV1 co-expressed in *Gal*⁺ mechanoheat nociceptor. The cKO of *Fxyd6* impaired the behavioral responses to noxious heat and intraplantar injection of capsaicin. The defects of thermal nociception in *Fxyd6* cKO mice were not mainly due to the loss of the regulatory effect of FXYD6 on Na^+ , K^+ -ATPase, because the responses to the noxious mechanical stimuli were not apparently altered in the mutant mice, and the physical blockage of the FXYD6/TRPV1 interaction could elevate the thermal threshold in wildtype of mice. Therefore, we provide an evidence that FXYD6 is involved in thermal nociception by interacting with TRPV1 channel in DRG neurons.

FXYD6 increases the TRPV1 activity in the specific type of DRG neurons

The single-cell RNA sequencing shows that *Trpv1* is mainly expressed in *Gal*⁺, *Sst*⁺ (C2 type) and

Mrgpra3⁺ (C4 type) DRG neurons that are also itch-sensing neurons,²¹ indicating that TRPV1 in different types of DRG neurons may have distinct functions. TRPV1-null mice and TRPV1-DTA mice lose the responses not only to heat, but also to pruritogenic chemical compounds.^{23,34,35} Actually, ablation of *Sst*⁺ DRG neurons or *Mrgpra3*⁺ neurons reduces the scratching behavior, but not change the thermal threshold.^{36,37} Re-introducing TRPV1 in *Mrgpra3*⁺ DRG neurons in TRPV1-null mice increases itch behavior, but little or no pain behavior.³⁶ Our present study demonstrates that FXYD6 could promote the thermal nociception and increase the activity of TRPV1 in DRG neurons, especially in *Gal*⁺ neurons. Therefore, we proposed that TRPV1 in *Gal*⁺ neurons played major role in the thermal nociception, while the TRPV1 in *Sst*⁺ and *Mrgpra3*⁺ neurons may play roles in the itch sensation. Moreover, many studies were performed to explore the regulation of TRPV1. What the TRPV1 regulators have in common is that they are widely distributed in DRG neurons, including Pirt, FGF13, SHANK3, β -arrestin-2 and calmodulin. The present study provides the evidence that FXYD6 could regulate TRPV1 channel precisely in the specific type DRG neurons, and promotes the thermal nociception.

PGDEE motif is required for the FXYD6/TRPV1 interaction and thermal nociception

In the present study, we found that FXYD6 interacted with TRPV1 channel and promoted thermal nociception. FXYD6 worked as a regulator of TRPV1 to increase the capsaicin-induced currents. Different regulators of TRPV1 usually binds the TRPV1, and further change the initial current of TRPV1 or desensitization of TRPV1. Membrane protein Pirt binds to TRPV1 via its positively charged C terminus, and further enhance activity of TRPV1.²⁷ SHANK3 interacts with TRPV1 via its proline-rich region, and regulates TRPV1.²⁹ KCHIP3 N-terminal 31–50 fragment binds to TRPV1, and decreases the surface localization of TRPV1.³⁸ Phosphorylation status of Thr³⁷⁰ in TRPV1 dictates the association of β -arrestin 2 and TRPV1, and β -arrestin 2 mediates the desensitization of TRPV1.²⁸ One study shows that calmodulin binds to the NH₂-terminal ANK1 domain of TRPV1, while another study shows that calmodulin could bind to the C-terminal ANK1 of TRPV1 and mediates the desensitization of TRPV1.^{26,39} Our present study identified the PGDEE motif of FXYD6 as a key site required for the FXYD6/TRPV1 interaction. The PGDEE motif is highly negatively charged, and completely conserved in all FXYD6 protein sequences of different species, suggesting the importance of PGDEE motif. Therefore, we proposed that the FXYD6/TRPV1 interaction was

mainly due to electrostatic interaction between the PGDEE motif of FXYD6 and the specific motif of TRPV1. Crystal structure of TRPV1 demonstrates that TRPV1 is a tetrameric protein and each monomer has six transmembrane segments.^{40,41} According to the structure of TRPV1 and FXYD1 (homologue of FXYD6), we speculated that the positively charged motif in ankyrin repeat domain of TRPV1 may participate in the FXYD6-TRPV1 interaction.^{42,43} Besides, we found that blocking the FXYD6/TRPV1 interaction could elevate the thermal threshold. Thus, the PGDEE motif of FXYD6 is not only required for the FXYD6/TRPV1 interaction, but also for the thermal nociception. Our study provides the evidence that FXYD6 promotes the thermal nociception through interacting with TRPV1 channel, suggesting its potential for pain therapy.

Author Contributions

X. Z., L. B., and K.-C. L. designed research; H. L., B. C., J. P. and H.-X. S. performed research; K.-K. W. provided single-cell RNAseq data; H. L. analyzed data; X. Z., L. B., K.-C. L. and H. L. wrote the paper.

Declaration of Conflicting Interests


The author(s) declared no potential conflicts of interest with respect to the research, authorship, and/or publication of this article.

Funding

The author(s) disclosed receipt of the following financial support for the research, authorship, and/or publication of this article: This work was supported by NNSFC (31630033 and 31671094), CAS (QYZDY-SSW-SMC007), SPRP (B) of CAS (XDB39000000), STCSM (18JC1420301) and CAMS Innovation Fund for Medical Sciences (2019-I2M-5-082).

ORCID iDs

Hao Luo  <https://orcid.org/0000-0002-3362-9687>

Kai-Cheng Li  <https://orcid.org/0000-0001-7732-3076>

References

1. Yamaguchi F, Yamaguchi K, Tai Y, Sugimoto K, Tokuda M. Molecular cloning and characterization of a novel phospholemman-like protein from rat hippocampus. *Brain Res Mol Brain Res* 2001; 86: 189–192.
2. Saito S, Matoba R, Kato K, Matsubara K. Expression of a novel member of the ATP1G1/PLM/MAT8 family, phospholemman-like protein (PLP) gene, in the developmental process of mouse cerebellum. *Gene* 2001; 279: 149–155.
3. Sweadner KJ, Rael E. The FXYD gene family of small ion transport regulators or channels: cDNA sequence, protein signature sequence, and expression. *Genomics* 2000; 68: 41–56.

4. Crambert G, Geering K. FXYP proteins: new tissue-specific regulators of the ubiquitous Na,K-ATPase. *Sci STKE* 2003; 2003: RE1.
5. Garty H, Karlish SJ. Role of FXYP proteins in ion transport. *Annu Rev Physiol* 2006; 68: 431–459.
6. Delprat B, Schaer D, Roy S, Wang J, Puel JL, Geering K. FXYP6 is a novel regulator of Na,K-ATPase expressed in the inner ear. *J Biol Chem* 2007; 282: 7450–7456.
7. Liu J, Zhou N, Zhang X. A monoclonal antibody against human FXYP6. *Hybridoma (Larchmt)* 2011; 30: 487–490.
8. Chen X, Sun M, Hu Y, Zhang H, Wang Z, Zhou N, Yan X. FXYP6 is a new biomarker of cholangiocarcinoma. *Oncol Lett* 2014; 7: 393–398.
9. Gao Q, Chen X, Duan H, Wang Z, Feng J, Yang D, Song L, Zhou N, Yan X. FXYP6: a novel therapeutic target toward hepatocellular carcinoma. *Protein Cell* 2014; 5: 532–543.
10. Yang Z, Chen Y, Fu Y, Yang Y, Zhang Y, Chen Y, Li D. Meta-analysis of differentially expressed genes in osteosarcoma based on gene expression data. *BMC Med Genet* 2014; 15: 80.
11. Choudhury K, McQuillin A, Puri V, Pimm J, Datta S, Thirumalai S, Krasucki R, Lawrence J, Bass NJ, Quedsted D, Crombie C, Fraser G, Walker N, Nadeem H, Johnson S, Curtis D, St Clair D, Gurling HM. A genetic association study of chromosome 11q22–24 in two different samples implicates the FXYP6 gene, encoding phosphohippolin, in susceptibility to schizophrenia. *Am J Hum Genet* 2007; 80: 664–672.
12. Iwata Y, Yamada K, Iwayama Y, Anitha A, Thanseem I, Toyota T, Hattori E, Ohnishi T, Maekawa M, Nakamura K, Suzuki K, Matsuzaki H, Tsuchiya KJ, Suda S, Sugihara G, Takebayashi K, Yamamoto S, Iwata K, Mori N, Yoshikawa T. Failure to confirm genetic association of the FXYP6 gene with schizophrenia: the Japanese population and meta-analysis. *Am J Med Genet B Neuropsychiatr Genet* 2010; 153: 1221–1227.
13. Zhong N, Zhang R, Qiu C, Yan H, Valenzuela RK, Zhang H, Kang W, Lu S, Guo T, Ma J. A novel replicated association between FXYP6 gene and schizophrenia. *Biochem Biophys Res Commun* 2011; 405: 118–121.
14. Mulligan MK, Ponomarev I, Hitzemann RJ, Belknap JK, Tabakoff B, Harris RA, Crabbe JC, Blednov YA, Grahame NJ, Phillips TJ, Finn DA, Hoffman PL, Iyer VR, Koob GF, Bergeson SE. Toward understanding the genetics of alcohol drinking through transcriptome meta-analysis. *Proc Natl Acad Sci U S A* 2006; 103: 6368–6373.
15. Delprat B, Puel JL, Geering K. Dynamic expression of FXYP6 in the inner ear suggests a role of the protein in endolymph homeostasis and neuronal activity. *Dev Dyn* 2007; 236: 2534–2540.
16. Shrestha BR, Chia C, Wu L, Kujawa SG, Liberman MC, Goodrich LV. Sensory neuron diversity in the inner ear is shaped by activity. *Cell* 2018; 174: 1229–1246.
17. Shindo Y, Morishita K, Kotake E, Miura H, Carninci P, Kawai J, Hayashizaki Y, Hino A, Kanda T, Kusakabe Y. FXYP6, a Na,K-ATPase regulator, is expressed in type II taste cells. *Biosci Biotechnol Biochem* 2011; 75: 1061–1066.
18. Maeda N, Onimura M, Ohmoto M, Inui T, Yamamoto T, Matsumoto I, Abe K. Spatial differences in molecular characteristics of the pontine parabrachial nucleus. *Brain Res* 2009; 1296: 24–34.
19. Basbaum AI, Bautista DM, Scherrer G, Julius D. Cellular and molecular mechanisms of pain. *Cell* 2009; 139: 267–284.
20. Marmigere F, Ernfors P. Specification and connectivity of neuronal subtypes in the sensory lineage. *Nat Rev Neurosci* 2007; 8: 114–127.
21. Li CL, Li KC, Wu D, Chen Y, Luo H, Zhao JR, Wang SS, Sun MM, Lu YJ, Zhong YQ, Hu XY, Hou R, Zhou BB, Bao L, Xiao HS, Zhang X. Somatosensory neuron types identified by high-coverage single-cell RNA-sequencing and functional heterogeneity. *Cell Res* 2016; 26: 83–102.
22. Tominaga M, Caterina MJ, Malmberg AB, Rosen TA, Gilbert H, Skinner K, Raumann BE, Basbaum AI, Julius D. The cloned capsaicin receptor integrates multiple pain-producing stimuli. *Neuron* 1998; 21: 531–543.
23. Caterina MJ, Leffler A, Malmberg AB, Martin WJ, Trafton J, Petersen-Zeitl KR, Koltzenburg M, Basbaum AI, Julius D. Impaired nociception and pain sensation in mice lacking the capsaicin receptor. *Science* 2000; 288: 306–313.
24. Matta JA, Ahern GP. Voltage is a partial activator of rat thermosensitive TRP channels. *J Physiol* 2007; 585: 469–482.
25. Caterina MJ, Schumacher MA, Tominaga M, Rosen TA, Levine JD, Julius D. The capsaicin receptor: a heat-activated ion channel in the pain pathway. *Nature* 1997; 389: 816–824.
26. Rosenbaum T, Gordon-Shaag A, Munari M, Gordon SE. Ca²⁺/calmodulin modulates TRPV1 activation by capsaicin. *J Gen Physiol* 2004; 123: 53–62.
27. Kim AY, Tang Z, Liu Q, Patel KN, Maag D, Geng Y, Dong X. Pirt, a phosphoinositide-binding protein, functions as a regulatory subunit of TRPV1. *Cell* 2008; 133: 475–485.
28. Por ED, Bierbower SM, Berg KA, Gomez R, Akopian AN, Wetsel WC, Jeske NA. β -Arrestin-2 desensitizes the transient receptor potential vanilloid 1 (TRPV1) channel. *J Biol Chem* 2012; 287: 37552–37563.
29. Han Q, Kim YH, Wang X, Liu D, Zhang ZJ, Bey AL, Lay M, Chang W, Berta T, Zhang Y, Jiang YH, Ji RR. SHANK3 deficiency impairs heat hyperalgesia and TRPV1 signaling in primary sensory neurons. *Neuron* 2016; 92: 1279–1293.
30. Yang L, Dong F, Yang Q, Yang PF, Wu R, Wu QF, Wu D, Li CL, Zhong YQ, Lu YJ, Cheng X, Xu FQ, Chen L, Bao L, Zhang X. FGF13 selectively regulates heat nociception by interacting with Na_v1.7. *Neuron* 2017; 93: 806–821.
31. Li KC, Zhang FX, Li CL, Wang F, Yu MY, Zhong YQ, Zhang KH, Lu YJ, Wang Q, Ma XL, Yao JR, Wang JY, Lin LB, Han M, Zhang YQ, Kuner R, Xiao HS, Bao L, Gao X, Zhang X. Follistatin-like 1 suppresses sensory afferent transmission by activating Na⁺,K⁺-ATPase. *Neuron* 2011; 69: 974–987.

32. Wang F, Cai B, Li KC, Hu XY, Lu YJ, Wang Q, Bao L, Zhang X. FXYD2, a γ subunit of Na^+ , K^+ -ATPase, maintains persistent mechanical allodynia induced by inflammation. *Cell Res* 2015; 25: 318–334.
33. Li KC, Wang F, Zhong YQ, Lu YJ, Wang Q, Zhang FX, Xiao HS, Bao L, Zhang X. Reduction of follistatin-like 1 in primary afferent neurons contributes to neuropathic pain hypersensitivity. *Cell Res* 2011; 21: 697–699.
34. Mishra SK, Tisel SM, Orestes P, Bhangoo SK, Hoon MA. TRPV1-lineage neurons are required for thermal sensation. *Embo J* 2011; 30: 582–593.
35. Imamachi N, Park GH, Lee H, Anderson DJ, Simon MI, Basbaum AI, Han SK. TRPV1-expressing primary afferents generate behavioral responses to pruritogens via multiple mechanisms. *Proc Natl Acad Sci U S A* 2009; 106: 11330–11335.
36. Han L, Ma C, Liu Q, Weng HJ, Cui Y, Tang Z, Kim Y, Nie H, Qu L, Patel KN, Li Z, McNeil B, He S, Guan Y, Xiao B, Lamotte RH, Dong X. A subpopulation of nociceptors specifically linked to itch. *Nat Neurosci* 2013; 16: 174–182.
37. Stantcheva KK, Iovino L, Dhandapani R, Martinez C, Castaldi L, Nocchi L, Perlas E, Portulano C, Pesaresi M, Shirlekar KS, de Castro Reis F, Paparountas T, Bilbao D, Heppenstall PA. A subpopulation of itch-sensing neurons marked by ret and somatostatin expression. *EMBO Rep* 2016; 17: 585–600.
38. Tian NX, Xu Y, Yang JY, Li L, Sun XH, Wang Y, Zhang Y. KChIP3 N-terminal 31-50 fragment mediates its association with TRPV1 and alleviates inflammatory hyperalgesia in rats. *J Neurosci* 2018; 38: 1756–1773.
39. Numazaki M, Tominaga T, Takeuchi K, Murayama N, Toyooka H, Tominaga M. Structural determinant of TRPV1 desensitization interacts with calmodulin. *Proc Natl Acad Sci U S A* 2003; 100: 8002–8006.
40. Liao M, Cao E, Julius D, Cheng Y. Structure of the TRPV1 ion channel determined by electron cryo-microscopy. *Nature* 2013; 504: 107–112.
41. Cao E, Liao M, Cheng Y, Julius D. TRPV1 structures in distinct conformations reveal activation mechanisms. *Nature* 2013; 504: 113–118.
42. Lishko PV, Procko E, Jin X, Phelps CB, Gaudet R. The ankyrin repeats of TRPV1 bind multiple ligands and modulate channel sensitivity. *Neuron* 2007; 54: 905–918.
43. Teriete P, Franzin CM, Choi J, Marassi FM. Structure of the Na,K-ATPase regulatory protein FXYD1 in micelles. *Biochemistry* 2007; 46: 6774–6783.